

Supplementary Information for

**A microfluidic DNA sensor array for real-time screening
early-stage lung cancer by simultaneous detection of
multiple miRNAs**

Jian Zhang,^a Wen Yao,^a Xuanjiao Mao,^{b*} Xinyu Hu,^a Li Lv^a and Haochen Qi^{a*}

^a College of Electrical and Electronic Engineering, Wenzhou University, Wenzhou 325035, China

^b Clinical Laboratory, The People's Hospital of Pingyang, Wenzhou 325400, China

Emails: haochenqi@wzu.edu.cn; pymxj@sina.com

Table S1 the sequences of miRNAs and aptamers

Oligonucleotide	Sequence (5'-3')
miR-221	AGC UAC AUU GUC UGC UGG GUU UC
DNA-221	GAA ACC CAG CAG ACA ATG TAG CT
miR-25	CAU UGC ACU UGU CUC GGU CUG A
DNA-25	TCA GAC CGA GAC AAG TGC AAT G
miR-222	AGC UAC AUC UGG CUA CUG GGU
DNA -222	ACC CAG TAG CCA GAT GTA GCT
miR-320a-3p	AAA AGC UGG GUU GAG AGG GCG A
DNA-320a-3p	TCG CCC TCT CAA CCC AGC TTT T
NC miRNA	UUG UAC UAC ACA AAA GUA CUG

Equation S1

$$u_{DEP} = \frac{r^2 \varepsilon_m}{6\eta} R_e[K(\omega)] \nabla |E|^2 = \frac{r^2 \varepsilon_m}{6\eta} R_e \left[\frac{\varepsilon_p^* - \varepsilon_m^*}{\varepsilon_p^* + 2\varepsilon_m^*} \right] \nabla |E|^2 \quad (\text{Eq. S1})$$

The DEP speed of a miRNA can be expressed as Eq. S1, where ε_m represents the permittivity of the solution, η represents its viscosity, and r is the radius of a given miRNA. $R_e \left[\frac{\varepsilon_p^* - \varepsilon_m^*}{\varepsilon_p^* + 2\varepsilon_m^*} \right]$ represents the real part of Clausius-Mossotti factor, ε_p^* and ε_m^* represent the complex forms of the the permittivities of miRNA and the solution, respectively, which can be expressed as $\varepsilon^* = \varepsilon - j \frac{\sigma}{\omega}$ (ε , σ , and ω represent the permittivity, conductivity and angular frequency). $\nabla |E|^2$ is the gradient of the square of electric field strength. The direction of DEP force is determined by $R_e[K(\omega)]$. When $R_e[K(\omega)] > 0$, the miRNA will move towards the IDE edge with high electric field strength due to the positive DEP force. When $R_e[K(\omega)] < 0$, it will move away from IDE due to the negative DEP force. In this work, positive DEP force will accelerate the movement of miRNAs towards the IDEs.

Equation S2

$$\frac{\Delta C}{C_{initial}} = \frac{C_{final} - C_{initial}}{C_{initial}} = -\lambda_{miRNA} \left/ \left(\lambda_{miRNA} + \frac{\varepsilon_{miRNA}}{\varepsilon_{APT}} \lambda_{APT} + \frac{\varepsilon_{miRNA}}{\varepsilon_{EDL}} \right) \right. \quad (\text{Eq. S2})$$

The change rate of the solid-liquid capacitance in the test duration is presented by Eq. S2, where $\Delta C = C_{final} - C_{initial}$, $C_{initial}$ is the initial and C_{final} is the final capacitances before and after detection of 30 s. λ_{miRNA} and λ_{APT} are the layer depths of miRNA and aptamer, respectively. ε is the permittivity, with the subscript characters representing miRNA, aptamer and EDL. According to this equation, the change rate of capacitance is negative after the target miRNAs are adsorbed on the IDE surface by

aptamers.

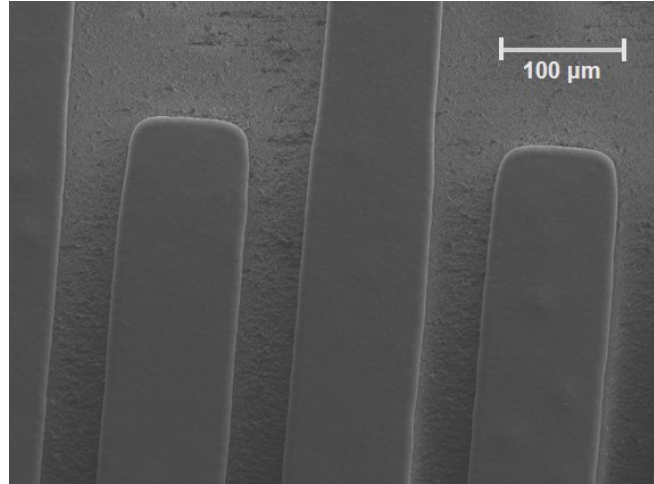


Fig. S1 SEM image of the IDE unit

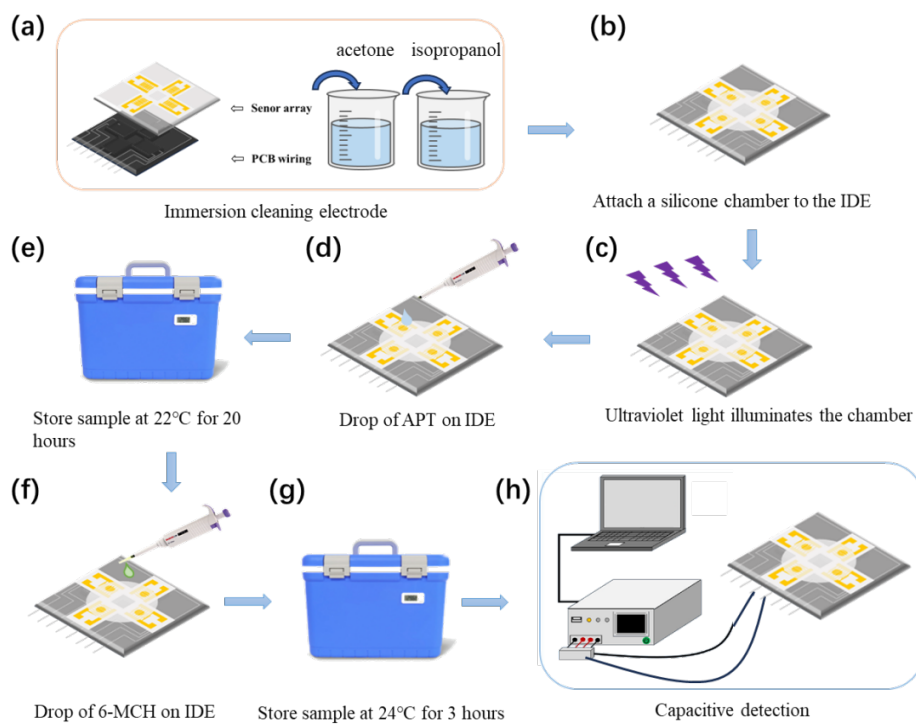


Fig. S2 Functionalization and detection of the sensor array

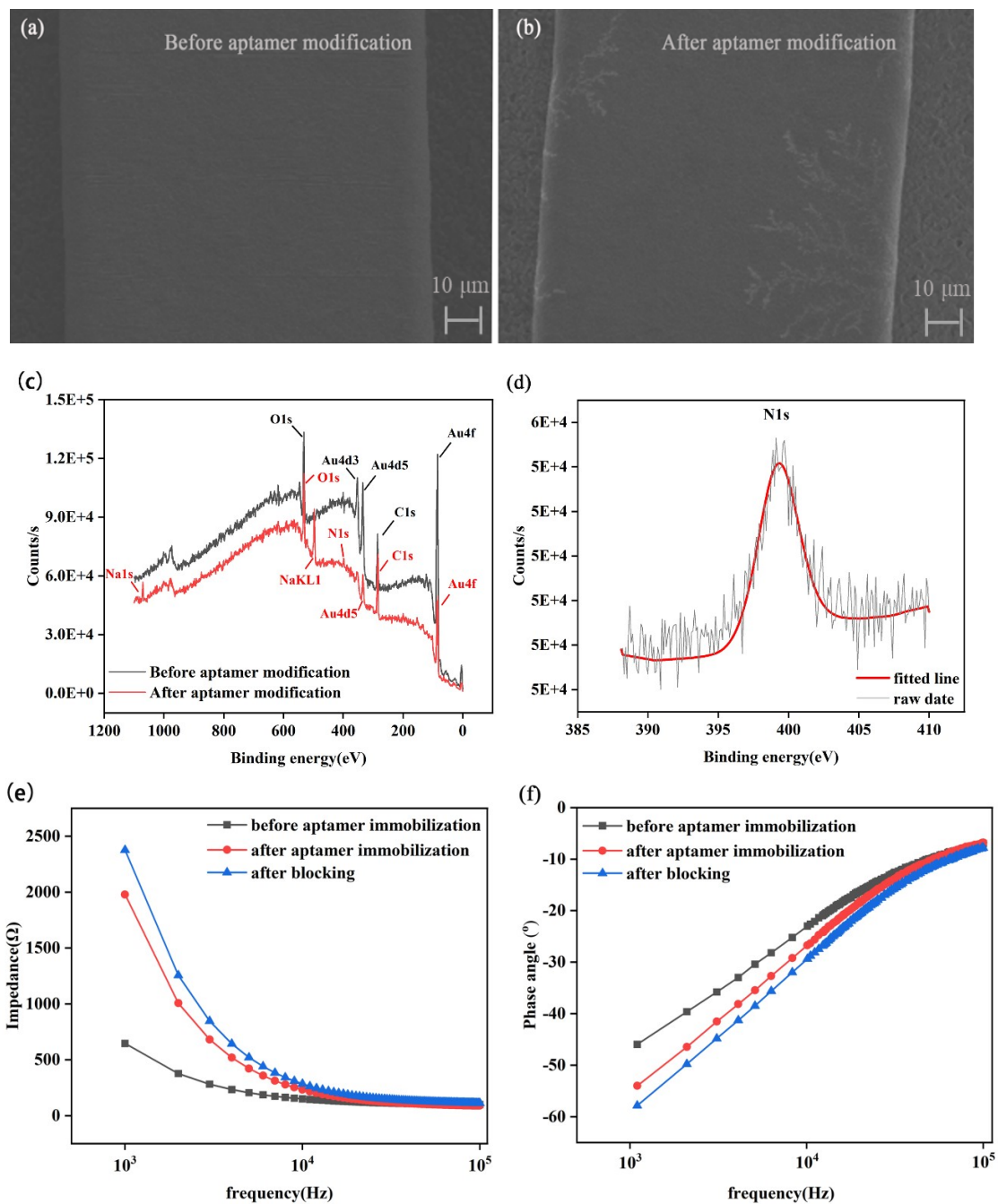


Fig. S3 SEM images of the IDE surface **(a)** before and **(b)** after DNA aptamer modification. **(c)** XPS spectrums of the IDE surface before and after DNA aptamer modification. **(d)** High resolution XPS spectrum of N element after DNA aptamer modification. **(e)** Impedance spectrum and **(f)** phase angle spectrum of the IDE-solution system from 10^3 to 10^5 Hz.

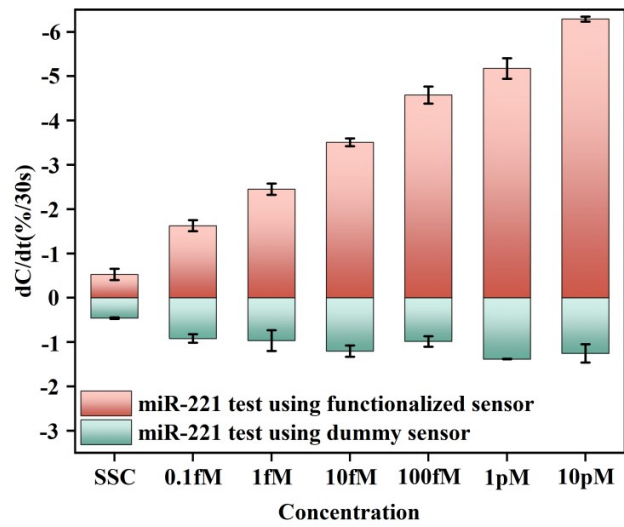


Fig. S4 Capacitance change rate from functionalized and dummy sensors in the presence of miR-221 with various concentrations. The dummy sensors are prepared with blocking but without aptamer.

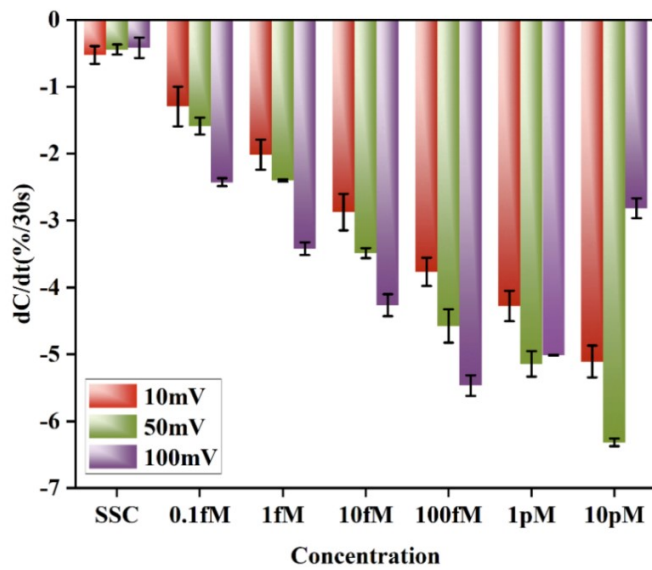


Fig. S5 Optimization of the detection voltage: dose response of capacitance change rate at different concentrations of miRNA-221 from 0.1 fM to 10 pM in 0.1×SSC under different voltage (10 mV, 50 mV and 100 mV).

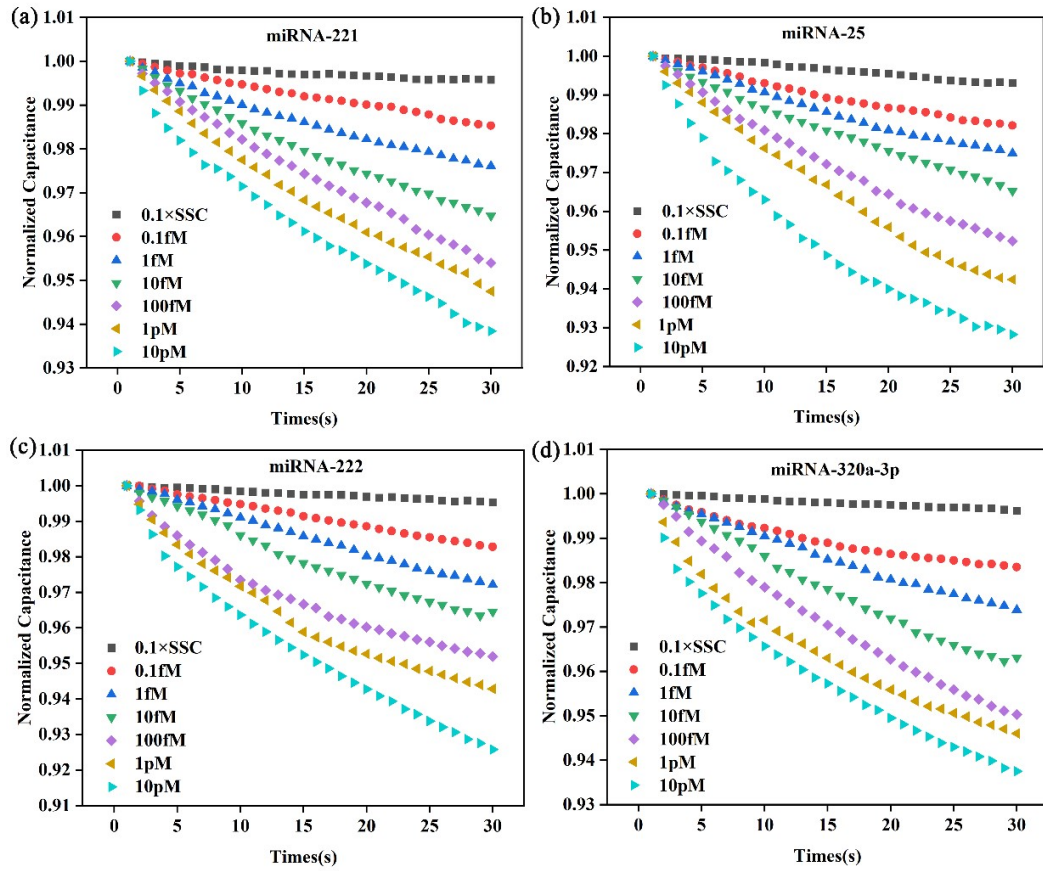


Fig. S6 Typical normalized transient response from 4 miRNAs (a: miR-221, b: miR-25, c: miR-222, d: miR-320a-3p) in 0.1xSSC.